Dynamics of bouncing-versus-merging response in jet collision

Minglei Li,[1,2] Abhishek Saha,[2] D. L. Zhu,[2] Chao Sun,[1,3] and Chung K. Law[1,2,*]
[1]*Center for Combustion Energy, Tsinghua University, Beijing 100084, China*
[2]*Department of Mechanical and Aerospace Engineering, Princeton University, Princeton, New Jersey 08544, USA*
[3]*Physics of Fluids Group, University of Twente, Enschede, Netherlands*
(Received 26 September 2014; revised manuscript received 8 May 2015; published 24 August 2015)

A new regime of oblique jet collision, characterized by low impact inertia and jet merging through bridge formation, is observed and thereby completes the entire suite of possible jet collision outcomes of (soft) merging, bouncing, and (hard) merging with increasing inertia. These distinct regimes, together with the observed dependence of the collision outcome on the impact angle and liquid properties, are characterized through scaling analysis by considering the competing effects of impact inertia, surface tension, and viscous thinning of the interfacial air gap leading to merging.

DOI: 10.1103/PhysRevE.92.023024 PACS number(s): 47.15.Uv, 47.60.Kz

I. INTRODUCTION

Collision of two fluid masses is a common natural and industrial phenomenon that occurs, for example, in cloud and raindrop formation, inkjet printing, insecticide spraying, and processes within liquid-fueled combustors such as diesel and rocket engines [1–8]. The most extensively investigated situation is perhaps the head-on collision between two identical droplets demonstrating [9,10] that with increasing impact inertia, represented by the collision Weber number (We), the droplets will (I) merge, (II) bounce, (III) merge again, and, finally, (IV) merge, followed by separation, with the concomitant production of secondary and even tertiary droplets (see Fig. 1 for the time-resolved images). Similar studies on the equally relevant problem of two colliding jets, however, have only shown [11,12] regimes analogous to regimes II, III, and IV but not regime I for merging at very low impact inertia. Such an absence is intriguing as it suggests the possibility that this regime actually may not exist as the correspondingly increased importance of the surface tension force under such low-inertia situations could inhibit either the generation and/or formation of steady jet. The present study has, however, successfully observed regime I behavior, with a bridge-enabled merging mechanism, and as such completed all possible regimes of the jet collision phenomenon. We shall present in the following our experimental investigation and results, analysis of the mechanisms governing the various regimes, and their dependence on the key system parameters of the impact inertia and orientation and properties of the fluid.

II. EXPERIMENTAL SETUP

The experimental apparatus consists of two identical nozzles whose relative positions and orientations can be individually manipulated by microrotation and *XYZ*-microposition stages, so that the collision configuration can be precisely controlled. The test fluid, drawn from a liquid reservoir, is pumped to the nozzles by two separate glass syringes driven by a double-channel syringe pump. The flow rate can be varied from 1.0 to 28.0 mL/min with an accuracy of $\pm 0.5\%$. The nozzles are stainless steel capillary tubes with 200 μm inner diameter. Technical grade *n*-alkanes, namely, *n*-decane, *n*-dodecane, *n*-tetradecane, and *n*-hexadecane, are used as the working fluids (properties are listed in Table I). High-precision pumps and positioners are used in order to generate and position the jets relevant for regimes I and II of low impact inertia. In particular, stable jets can be generated only slightly beyond the transition boundary into regime I, as further reduction of the jet inertia will lead to the break up of the jet into droplets (Rayleigh-Plateau instability) as surface tension becomes progressively more important. This is perhaps the reason that regime I has not been observed before.

III. RESULTS AND DISCUSSION

Mechanistically, the critical element governing merging versus bouncing of two colliding fluid masses is the dynamics and thickness of the gas gap separating the colliding interfaces [13–15] and whether the dimension of this gap can be reduced to that of the intermolecular van der Waals force of a few hundreds of nanometers so that the interfaces can attract and subsequently merge with each other. In the present study, we impinged the jets at various velocities and collision angles and recorded the images of the resulting collision configuration and outcome. Figures 2(I) to 2(IV) show a representative complete set of the nonmonotonic response of the colliding jets with increasing jet velocity V and hence impact inertia, with the collision angle α [half angle between the jets; see Fig. 2(a)] fixed at 30°. It is seen that, when the jet velocity is very small [(Fig. 2(I)], the jets merge with a "bridge" which pulls and links them by surface tension. This is the *missing* regime I that we have now observed, which we shall designate as "soft merging." With increasing velocity, the main panel of Fig. 2(II) together with the zoomed image of the contact zone in the inset shows that the jets bounce off upon collision without merging. If the velocity is further increased, the jets merge again and subsequently form a "chain" structure, as shown in Fig. 2(III). This regime is designated as "hard merging." Finally, with further increase in the jet velocity, the merged jet forms a liquid sheet which eventually breaks up, as shown in Fig. 2(IV). Since the chain structure and the associated breakup mechanism have been well investigated [12], we shall focus our subsequent exposition on the largely unexplained nonmonotonic behavior

*cklaw@princeton.edu

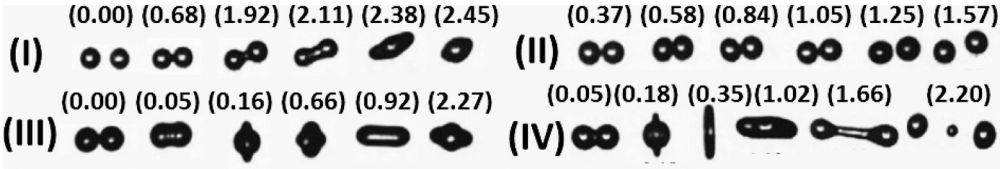

FIG. 1. Time-resolved imaging (time stamps in ms are in brackets) of head-on collisions of hydrocarbon droplets in 1 atm air: (I) regime I, soft merging, We = 0.2; (II) regime II, bouncing, We = 0.5; (III) regime III, hard merging, We = 32.8; and (IV) regime IV, separation after merging, We = 61.4. (Abstracted from Qian and Law [10]. Here the Weber number (We) is defined as $\mathrm{We} = (2\rho_l U^2 R)/\sigma$, where U is the relative velocity between the impacting droplets, R is the droplet radius, ρ_l is the liquid density, and σ is the surface tension.)

transitioning from soft merging through bouncing to hard merging, namely, regimes I, II, and III.

Discussion of the above nonmonotonic merging-bouncing-merging response can be facilitated by considering the roles of the head-on ($V \sin\alpha$) and parallel ($V \cos\alpha$) components of the impact velocity V, which bring the jets close while simultaneously entraining an air layer over the surfaces of the jets into the interfacial gap between them. Furthermore, as the jets approach each other, their interfaces are deformed and enlarged as the entrained air is squeezed by the head-on component of the impact inertia, leading to the concomitant increase in pressure in the interfacial region. The combined effects of increased interfacial area and pressure within the gap increase the repulsive force acting on the interfaces, causing the jets to slow down in the head-on direction. Simultaneously, some of the kinetic energy of the impact is converted to surface energy required to sustain the deformed surface, as well as viscously dissipated through the internal motion within the jets generated by their dynamics and deformation. If the head-on momentum is sufficiently large that the impacting interfaces can reach the distance at which the molecular attraction force becomes effective, then merging will take place. If, however, the jets lose all their head-on momentum before they can reach this distance, then they will bounce away, with the interfacial pressure relaxing and the deformed jets regaining their circular cross section. Since the jets have viscously lost some of their initial energy, the head-on momentum of the rebouncing jets is necessarily reduced from their impacting value such that the angle between the rebouncing jets is reduced from that of the impacting jets [$\alpha > \beta$ in Fig. 2(a)]. In the event of merging, the excess impact inertia and the surface energy resulting from the destruction of the interfaces will be partly or completely dissipated through the internal motion of the merged jet. Furthermore, the cross section of both the merged and bounced jets will oscillate between "prolate and oblate" from the circular shape once it is deformed [see Fig. 2(b) for a bounced jet event], similar to the classical problem of the oscillation of a droplet upon deformation analyzed in, for example, Lamb [16]. This oscillation generates additional internal motion and hence viscous dissipation within the jets.

TABLE I. Properties of the liquids used for the study.

Fluid	ρ(kg/m^3)	μ (10^{-3} Ns/m^2)	σ (mN/m)
Decane	730	0.92	23.80
Dodecane	750	1.34	25.35
Tetradecane	760	2.30	24.47
Hexadecane	773	3.00	28.12

Based on the above consideration, it is then clear that, for low impact velocities [Fig. 2(I)], flattening of the jet interface and internal viscous loss are both minimal, while the slow motion of approach allows the ready displacement of the interfacial gas, all of which allow the jet interfaces to approach within the molecular attraction distance to effect (soft) merging. In this regime, the jets lack sufficient impact inertia to cause strong jet deformation. With increasing velocity [Fig. 2(II)], all of the above favorable conditions for merging are compromised, leading to the complete loss of the head-on momentum before the interfaces can molecularly attract each other, hence leading to bouncing. Yet with still further increase in the jet velocity [Fig. 2(III)], the impact inertia dominates over other factors, causing (hard) merging. The merged jet may or may not remain intact depending on how readily the excess internal energy can be viscously dissipated through shape oscillation. It is also evident that the mechanisms for the soft and hard merging at low and high impact inertia are distinctly different. With low inertia the jets approach each other *gently,* and at one instant the molecular attraction force between the interfaces of the two jets becomes dominant and pulls the interfaces together. This creates the bridge-like structure with a sudden bend of the jet very close to the merging point, obviating the original direction of the impacting jets. At high impact inertia, however, the jets deform due to the interfacial pressure and approach each other rather strongly, maintaining their original directionality upon impact, with the intermolecular force playing a functioning but not dominant role for merging, and therefore, the prominent large-scale bridge does not form. The above description of the nonmonotonic jet collision responses spanning regimes I through IV then qualitatively corresponds to those of droplet collision and as such unifies the description of these two distinct collision phenomena.

We have also found that these merging-versus-bouncing mechanisms can, in addition, distinctively and richly manifest their influence through the two most important system parameters characterizing jet collision, namely, the collision angle α and properties of the fluid. These findings are demonstrated in Figs. 3(a)–3(d), which show the transition boundaries of soft and hard merging for the impact velocity V versus α for n-hexadecane, n-tetradecane, n-dodecane and n-decane, respectively.

Figure 3 shows that the soft merging transition boundary is insensitive to α, having an almost constant impact velocity. This therefore substantiates the physical interpretation mentioned earlier in that, due to the very low impact velocity and

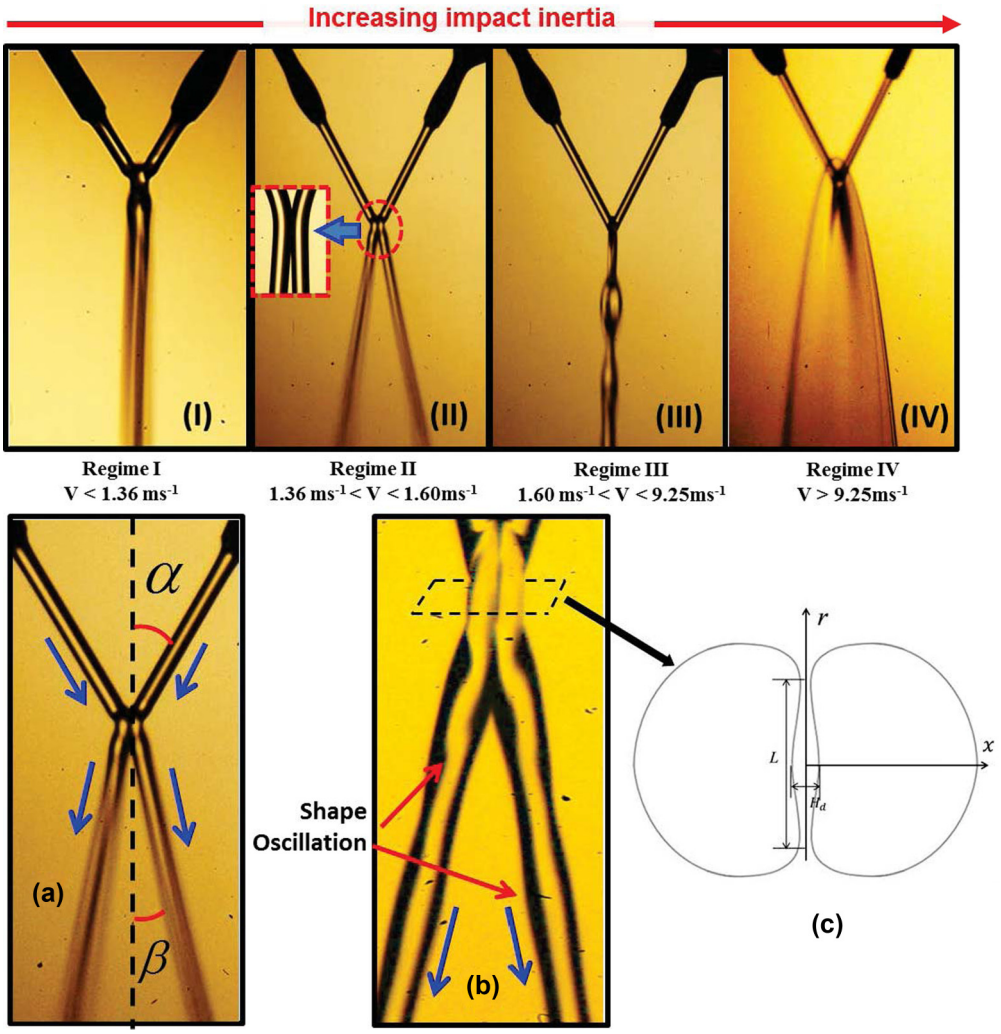

FIG. 2. (Color online) (I)–(IV) Images showing the complete suite of the collision response with increasing collision velocity (or impact inertia): (I) merging, (II) bouncing (inset: zoomed view of the interface), (III) merging (with subsequent chain structure), and (IV) merging followed by sheet formation and further breakup. Liquid: n-hexadecane; pressure: 1 bar. (a) Viscous loss through internal motion results in a smaller angle between bounced jets. Blue arrows show the direction of motion; a is the impact angle, and β is the rebound angle. (b) Shape oscillation of the bounced jets. (c) Sketch of the jet cross-section deformation and dimple formation. The deformation is not drawn to scale: the height of the dimple is much less than the dimple width.

the gentle nature of the impact, interfacial molecular attraction dominates merging through the formation of the connecting bridge and as such obviates the directionality of the impact. Such a bridge is equivalent to the "neck" formation during the merging of two droplets with minimal to no deformation and small impact inertia [17–19]. Mechanistically, when two undeformed circular surfaces meet, generally, they coalesce at a point and thus form an infinitely sharp curvature, leading to strong capillary pressure which spreads this point contact radially outward to facilitate the merging of two liquid masses into one. During this process, a fluid connection (neck or bridge) is formed between the two liquid bodies.

Contrary to soft merging, the hard merging transition boundary is expected to have a stronger dependence on the impact angle, which is indeed shown in Fig. 3. The fact that hard merging is promoted with increasing α can be appreciated by recognizing that the head-on impact inertia is increased through the increase in the normal component of the jet velocity, $V \sin\alpha$, and that the amount of entrained air over the jet surface is also correspondingly reduced through the reduced tangential motion, $V \cos\alpha$. Furthermore, since the two jets will always merge in the limit of head-on collision ($\alpha = 90^\circ$) because they are continuously directed towards each other and as such there is no gas film to separate the interfaces, one would expect that a critical angle beyond which merging is always possible should exist. Figure 3 shows that hard merging indeed becomes progressively favored as α increases, with a maximum α at which the soft and hard boundaries merge. This maximum α is 44°, 38°, 28°, and 19° for n-hexadecane, n-tetradecane, n-dodecane, and n-decane, respectively.

In order to understand the physical mechanism of the soft and hard transitions, we analyze the above experimental results from different n-alkanes which have similar van der Waals force but different fluid properties such as density, surface tension and viscosity. We first focus on the hard transition and examine the role of the air flow that moves with the

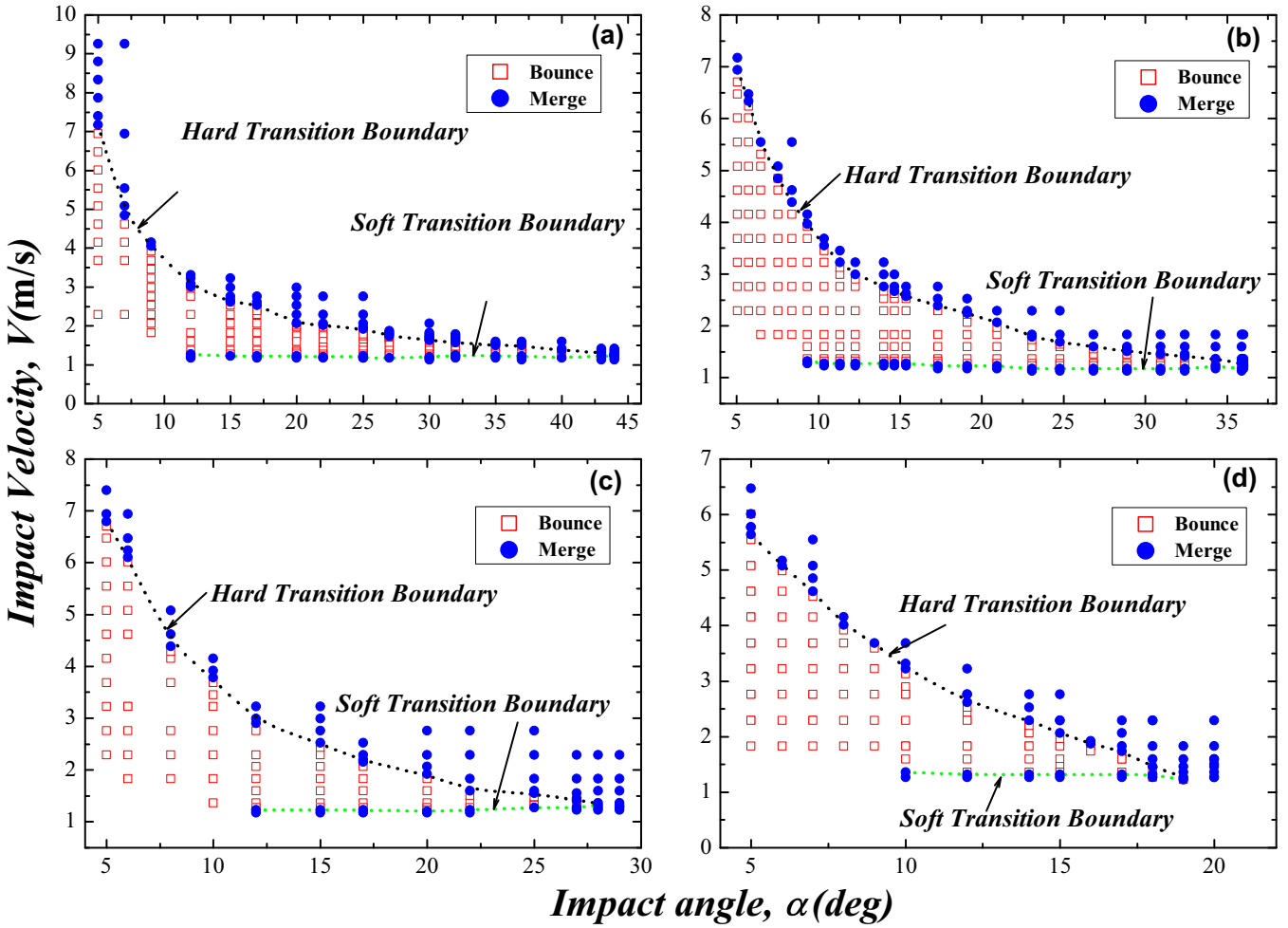

FIG. 3. (Color online) Quantitative regime boundaries of (a) n-hexadecane, (b) n-tetradecane, (c) n-dodecane, and (d) n-decane, showing the similar trend.

jets due to viscous drag. Although bouncing of the steady jets is sustained by the continuous supply of air, the disparity between the relative length scales, namely, the boundary layer thickness of the air, which is of the order of hundreds of microns, and the interfacial gap, which is of the order of microns, rules out any significant role of the air flow along the jet direction on the transition between bouncing and merging. Therefore, the tangential motion of the air flow, parallel to the jet direction, can be neglected. We therefore focus on the air flow in the plane that is normal to the jet direction, which can be simplified as an infinitesimally thin cross section of the jet that resembles a two-dimensional droplet, as sketched in Fig. 2(c). The entrapped air is strongly squeezed when the jets are approaching, resulting in a pressure buildup in the air gap between them. The elevated pressure in the air layer induces a dimple at the air-liquid interface, which is the key physical reason for the appearance of the bouncing regime. Merging can be effected only when the distance between the crests of the dimples is small enough that the van der Waals force starts to become important and destabilizes the air film [20,21]. Considering the inherent symmetry of the problem, the dynamics of the air layer between the colliding jets in the present case is analogous to that of the droplet impact on solid surfaces [22–24]. In those studies, the width of the air layer H_d scales with the dimensionless impact velocity as $H_d/R = A_I \mathrm{St}^{-2/3}$ for the inertia dominant regime, where St is the Stokes number, $\mathrm{St} = (\rho_l RU)/\eta_g$; A_I is a prefactor; ρ_l is the liquid density; R is the jet radius; η_g is the air viscosity; and U is the effective impact velocity, which is $V \sin\alpha$ in the present case. We further estimate the critical Stokes number value $\mathrm{St}_{\mathrm{trans}}$ at which the transition from bouncing to merging occurs. It has been shown that the molecular van der Waals forces become important when the distance between the liquid surfaces is reduced to ~200 nm [20,21]. Naturally, for merging to occur, the total air layer thickness $2H_d$ has to be smaller than this value. Using $H_d = 100\,\mathrm{nm}$ and $R = 100\,\mu\mathrm{m}$, we obtain $\mathrm{St}_{\mathrm{trans}} = 2.7 \times 10^3$ for the hard transition (see Supplemental Material for details [25]).

In contrast to hard transition, soft transition occurs at low jet velocities, at which capillary effects are important. In fact, as shown in Fig. 3, this transitional velocity does not depend on the jet orientation, namely, α. A close look at this soft transition in Fig. 3 shows that the transition from bouncing to merging always occurs at $V \sim 1\,\mathrm{m/s}$, which is close to the velocity of the capillary waves traveling along the jet, estimated as $V_c \approx (\sigma k/\rho_l)^{1/2} \approx 0.5\,\mathrm{m/s}$, where k is the wave number and is of the order of $1/R$. In the low-velocity case ($V < V_c$), the jet is not in a cylindrical shape due to the reflected waves to the nozzle.

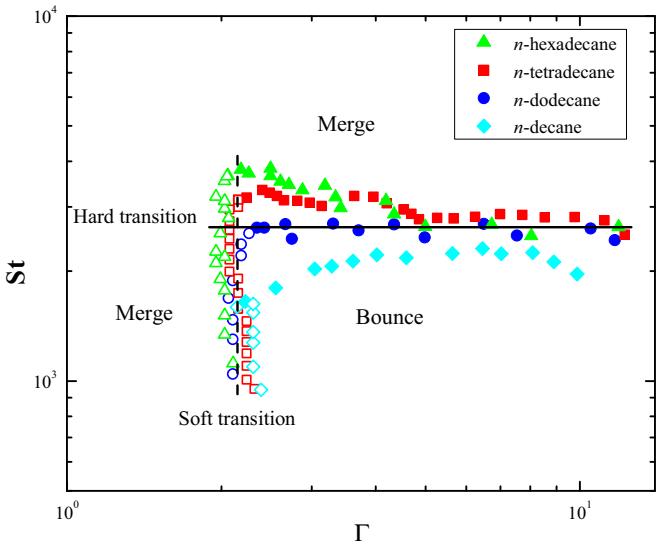

FIG. 4. (Color online) Soft transition (open symbols) and hard transition (solid symbols) boundaries on a St-Γ map. St is the Stokes number, $\mathrm{St} = (\rho_l R U)/\eta_g$; Γ is the velocity ratio, $\Gamma = V/V_c = V(\rho_l R/\sigma)^{1/2}$, where U is the effective impact velocity, $U = V \sin\alpha$, V is the jet velocity, α is the half angle between the jets, R is the jet radius, ρ_l is liquid density, η_g is gas viscosity, and σ is the surface tension.

In fact, these capillary waves are even visible in Fig. 2(b). However, the jets are continuous and do not break into droplets before the collision in our experiments. The remnant capillary waves on the surface change the shape of the jet at low velocity and bring segments of the jets close enough to effect the van der Waals force to cause merging. The ratio of jet velocity and capillary waves leads to a second nondimensional number, the velocity ratio, $\Gamma = V/V_c = V(\rho_l R/\sigma)^{1/2}$, which controls the soft transition.

Now, based on the above analyses of the two regimes controlled by the two nondimensional parameters St and Γ, in Fig. 4 we present the data on an St-Γ map. The solid symbols in Fig. 4 represent the transition Stokes number ($\mathrm{St}_{\mathrm{trans}}$) for hard merging and show that the data for different liquids largely collapse within a narrow horizontal regime around a critical St (2.7×10^3 with a prefactor $A_I = 0.19$), as expected from the scaling analysis above. The scatter close to the critical point, where hard and soft transition lines meet, could result from viscous dissipation of the jets, which has not been included in this simplified scaling argument. The open symbols in Fig. 4 represent the velocity ratio of the jets at the boundary of the soft merging transition and show that the transition velocity ratio for the different liquids also collapses to a tight regime of the order of unity, suggesting that this transition is indeed related to the effects of the capillarity of the jets. Consequently, the present results demonstrate that bouncing is confined to regimes of high velocity ratio Γ and low St, which represent weak capillary and weak impact inertia effects, respectively. It is then reasonable to expect that, due to the strong dependence on liquid properties such as surface tension and density, such regimes may not exist for some liquids. For example, at atmospheric conditions we did not observe bouncing for water, which has a high surface tension compared to those of the hydrocarbons.

IV. SUMMARY

In summary, we have conclusively demonstrated that jet collision exhibits nonmonotonic merging and bouncing behaviors with impact inertia, and these behaviors sensitively depend on the impact orientation and the properties of the liquid. Understanding gained herein offers rich options for practical applications. For example, the design of low-thrust satellite positioners using hypergolic fuels, which depends on jet mixing and liquid-phase reaction, can be extended to ultralow values of fine thrust. The operation of bipropellant rockets can also be controlled through vectoring of the injectors, particularly in response to the incipient onset of acoustic combustion instability within the chamber. Furthermore, combustion synthesis through jet mixing offers options for the large-scale production of novel materials of high purity, with the synthesis processes optimized by manipulating the various collision parameters identified herein.

[1] W. C. Macklin and P. V Hobbs, Subsurface phenomena and the splashing of drops on shallow liquids, Science **166**, 107 (1969).

[2] B. Ching, M. W. Golay, and T. J. Johnson, Droplet impacts upon liquid surfaces, Science **226**, 535 (1984).

[3] E. Bodenschatz, S. P. Malinowski, R. A. Shaw, and F. Stratmann, Can we understand clouds without turbulence?, Science **327**, 970 (2010).

[4] V. Bergeron, D. Bonn, J. Martin, and L. Vovelle, Controlling droplet deposition with polymer additives, Nature (London) **405**, 772 (2000).

[5] G. Falkovich, A. Fouxon, and M. G. Stepanov, Acceleration of rain initiation by cloud turbulence, Nature (London) **419**, 151 (2002).

[6] I. V. Roisman and C. Tropea, Impact of a drop onto a wetted wall: Description of crown formation and propagation, J. Fluid Mech. **472**, 373 (2002).

[7] T. Tran, H. De Maleprade, C. Sun, and D. Lohse, Air entrainment during impact of droplets on liquid surfaces, J. Fluid Mech. **726**, R3 (2013).

[8] C. K. Law, *Combustion Physics* (Cambridge University Press, New York, 2006).

[9] Y. J. Jiang, A. Umemura, and C. K. Law, An experimental investigation on the collision behaviour of hydrocarbon droplets, J. Fluid Mech. **234**, 171 (1992).

[10] J. Qian and C. K. Law, Regimes of coalescence and separation in droplet collision, J. Fluid Mech. **331**, 59 (1997).

[11] N. Wadhwa, P. Vlachos, and S. Jung, Noncoalescence in the Oblique Collision of Fluid Jets, Phys. Rev. Lett. **110**, 124502 (2013).

[12] J. W. M. Bush and A. E. Hasha, On the collision of laminar jets: Fluid chains and fishbones, J. Fluid Mech. **511**, 285 (2004).

[13] G. D. M. Mackay and S. G. Mason, The gravity approach and coalescence of fluid drops at liquid interfaces, Can. J. Chem. Eng. **41**, 203 (1963).
[14] E. D. Manev and A. V Nguyen, Critical thickness of microscopic thin liquid films, Adv. Colloid Interface Sci. **114**, 133 (2005).
[15] P. Zhang and C. K. Law, An analysis of head-on droplet collision with large deformation in gaseous medium, Phys. Fluids **23**, 042102 (2011).
[16] H. Lamb, *Hydrodynamics* (Cambridge University Press, New York, 1932).
[17] R. W. Hopper, Coalescence of two equal cylinders: Exact results for creeping viscous plane flow driven by capillarity, J. Am. Ceram. Soc. **67**, C-262 (1984).
[18] J. Eggers, J. R. Lister, and H. A. Stone, Coalescence of liquid drops, J. Fluid Mech. **401**, 293 (1999).
[19] J. D. Paulsen, J. C. Burton, S. R. Nagel, S. Appathurai, M. T. Harris, and O. A. Basaran, The inexorable resistance of inertia determines the initial regime of drop coalescence, Proc. Natl. Acad. Sci. USA **109**, 6857 (2012).
[20] Y. Couder, E. Fort, C. H. Gautier, and A. Boudaoud, From Bouncing to Floating: Noncoalescence of Drops on a Fluid Bath, Phys. Rev. Lett. **94**, 177801 (2005).
[21] S. T. Thoroddsen, M. J. Thoraval, K. Takehara, and T. G. Etoh, Micro-bubble morphologies following drop impacts onto a pool surface, J. Fluid Mech. **708**, 469 (2012).
[22] P. D. Hicks and R. Purvis, Air cushioning in droplet impacts with liquid layers and other droplets, Phys. Fluids **23**, 062104 (2011).
[23] W. Bouwhuis, R. C. A. van der Veen, T. Tran, D. L. Keij, K. G. Winkels, I. R. Peters, D. van der Meer, C. Sun, J. H. Snoeijer, and D. Lohse, Maximal Air Bubble Entrainment at Liquid-Drop Impact, Phys. Rev. Lett. **109**, 264501 (2012).
[24] E. Klaseboer, R. Manica, and D. Y. C. Chan, Universal Behavior of the Initial Stage of Drop Impact, Phys. Rev. Lett. **113**, 194501 (2014).
[25] See Supplemental Material at http://link.aps.org/supplemental/10.1103/PhysRevE.92.023024 for details of experimental setup and calculations.